

## Supporting Information

### **Fiber-based multifunctional nickel phosphide electrodes for flexible energy conversion and storage**

Zheye Zhang, Shasha Liu, Jian Xiao and Shuai Wang\*

Z. Y. Zhang, S. S. Liu, J. Xiao, Prof. S. Wang

School of Chemistry and Chemical Engineering, Huazhong University of Science and Technology, Wuhan 430074, P. R. China

\*E-mail: [chmsamuel@mail.hust.edu.cn](mailto:chmsamuel@mail.hust.edu.cn)

## 1. Supplementary Figures



**Figure S1.** Photograph of CF (left) and CF@Ni (right).

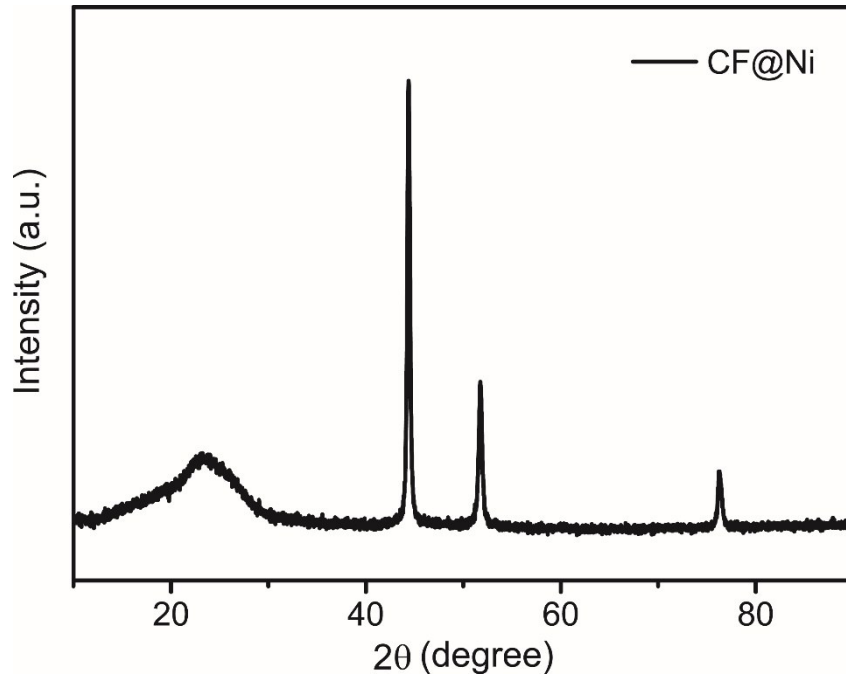


**Figure S2.** XRD pattern of CF@Ni.

This XRD pattern shows three strong peaks located at  $44.8^\circ$ ,  $52.1^\circ$  and  $76.6^\circ$ , which can be indexed to the (111), (200), and (220) planes, respectively, indicating the formation of metallic Ni. While the peak located at  $23.4^\circ$  corresponds to CF.

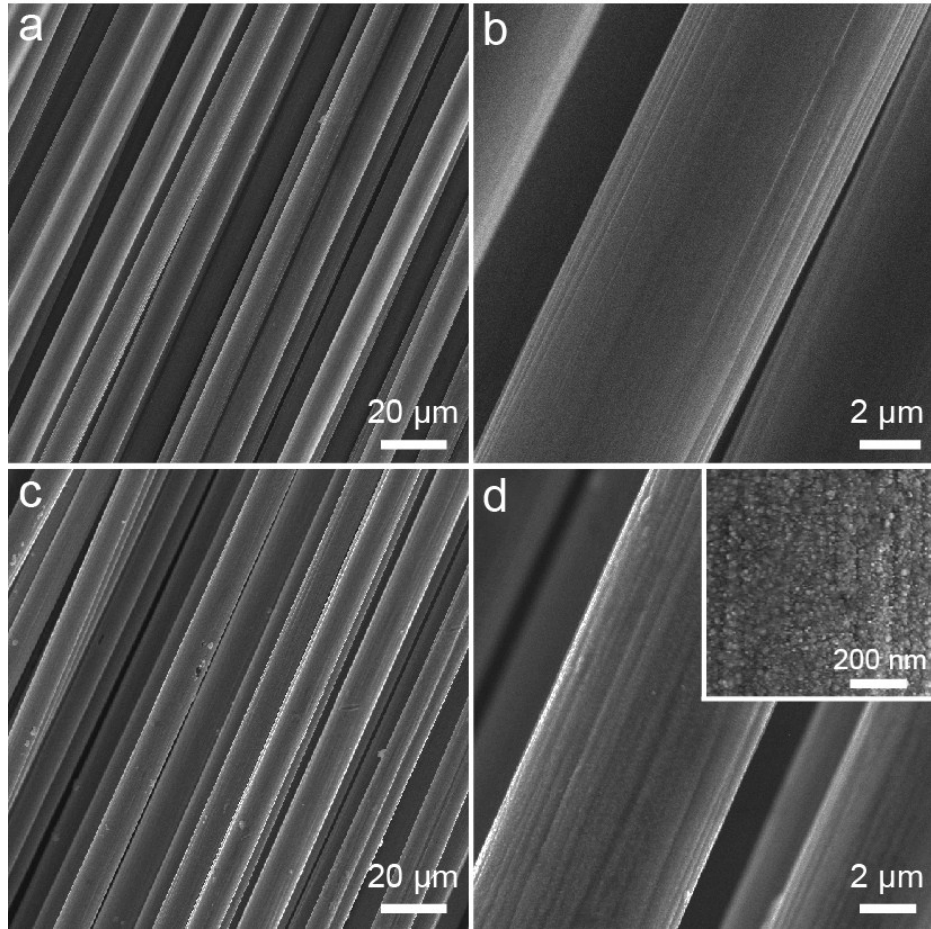


**Figure S3.** SEM images of a,b) CF and c,d) CF@Ni.

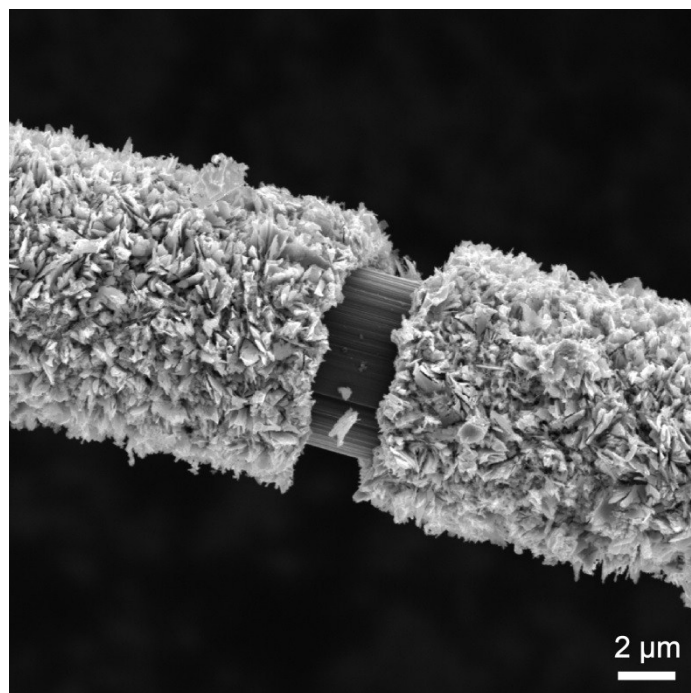


**Figure S4.** SEM image of a broken CF@NiP<sub>x</sub>.

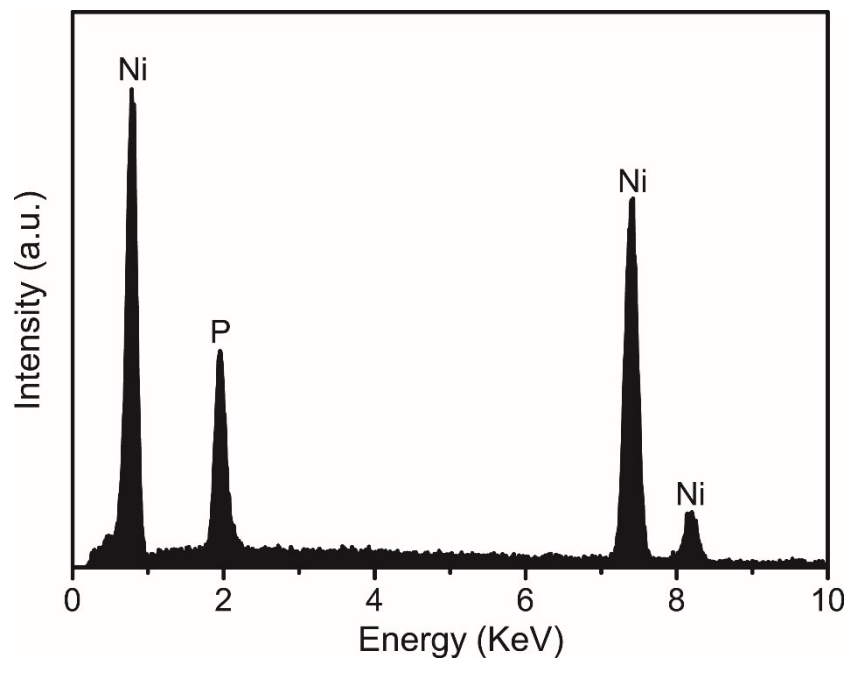


**Figure S5.** EDX spectrum of CF@NiP<sub>x</sub>.

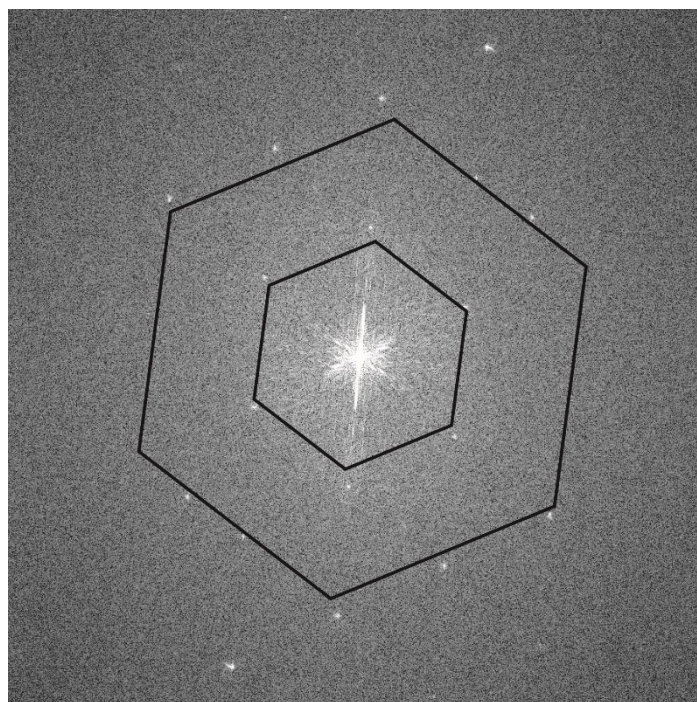


**Figure S6.** FFT pattern of the Ni<sub>2</sub>P hexagonal structure.

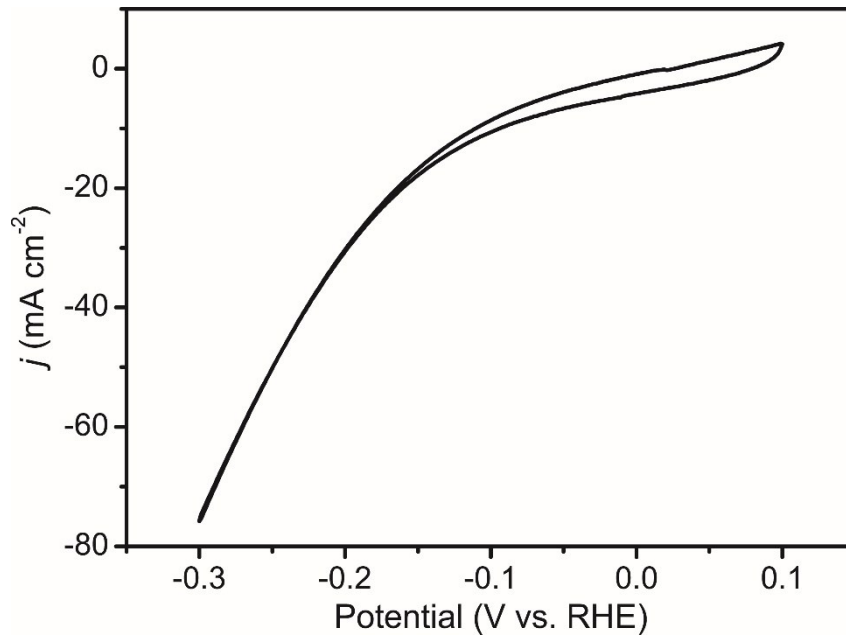


**Figure S7.** CV cycling test for CF@NiP<sub>x</sub> with a scan rate of 5 mV s<sup>-1</sup> for HER in 1.0 M KOH.

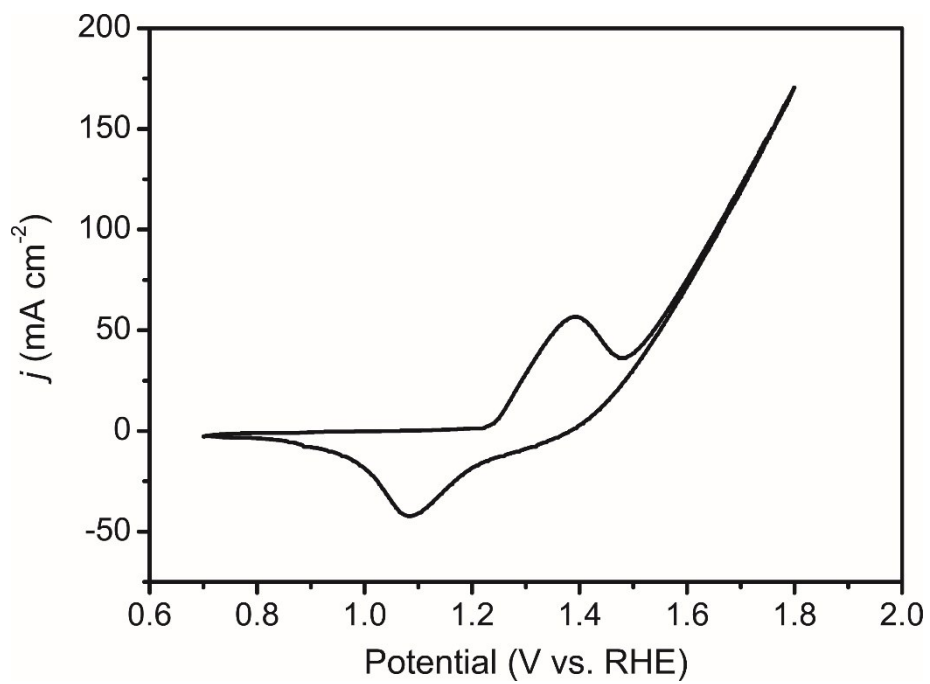


**Figure S8.** CV cycling test for CF@NiP<sub>x</sub> with a scan rate of 5 mV s<sup>-1</sup> for OER in 1.0 M KOH.

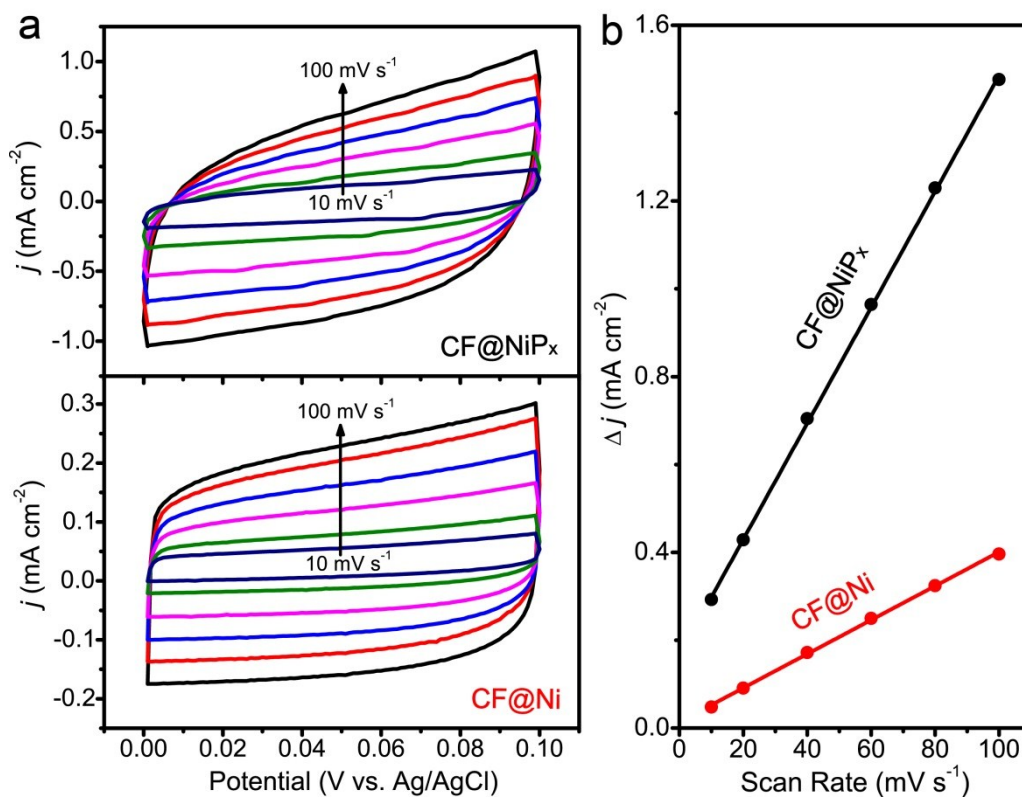


**Figure S9.** a) CV curves of CF@NiP<sub>x</sub> and CF@Ni electrodes with various scan rates. b) The charging current density differences plotted against scan rates for CF@NiP<sub>x</sub> and CF@Ni. The linear slope, equivalent to twice the  $C_{dl}$ , was employed to represent the ECSA.

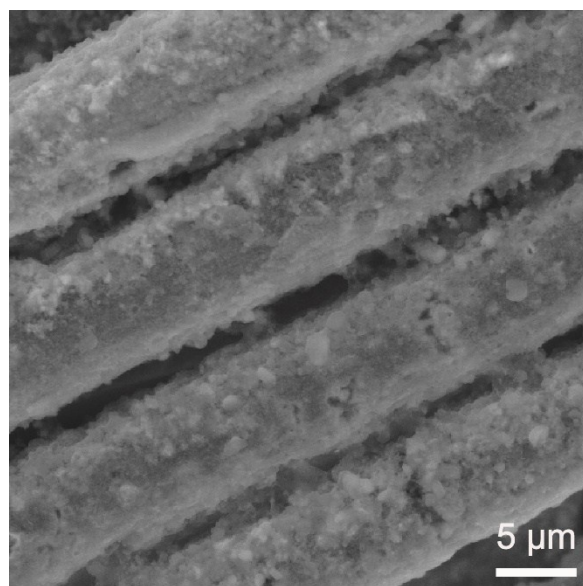


**Figure S10.** SEM image of the CF@NiP<sub>x</sub> catalyst after a 12 h OER stability test.

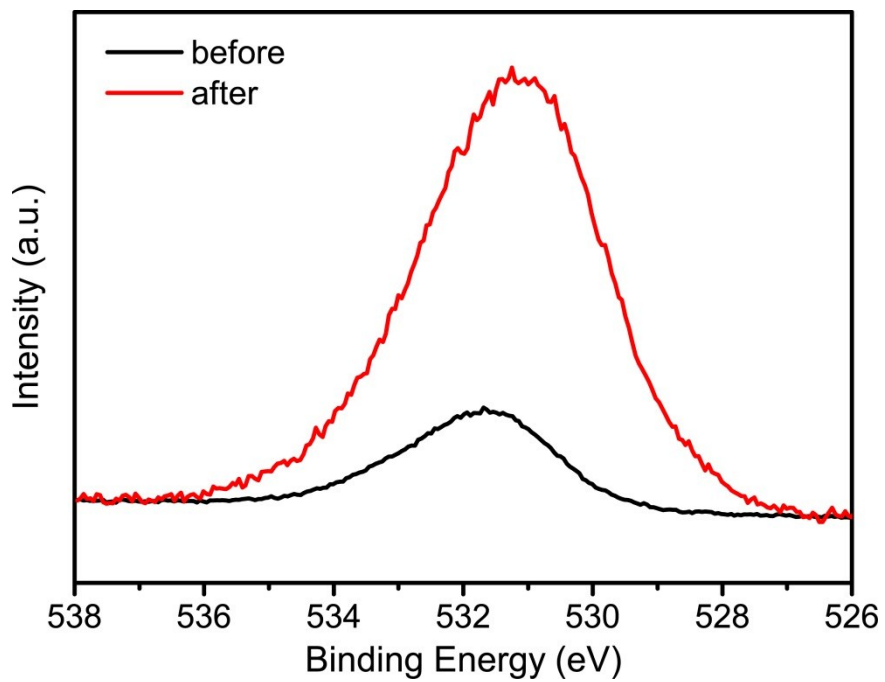


**Figure S11.** O 1s XPS spectra for the fresh and post-OER CF@NiP<sub>x</sub> electrocatalyst.

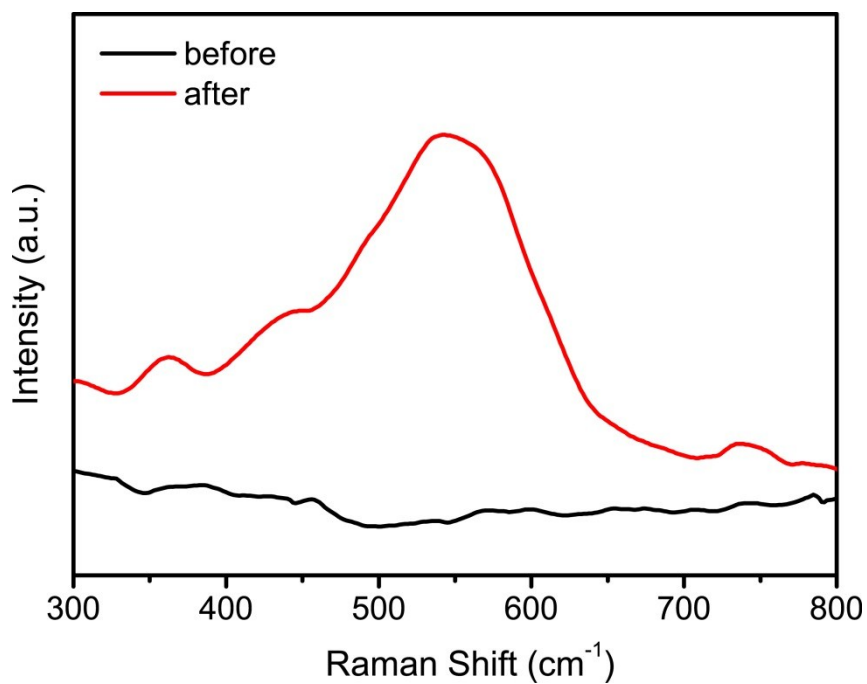


**Figure S12.** Raman spectra for the fresh and post-OER CF@NiP<sub>x</sub> electrocatalyst.

Additional proof of the formation of higher oxides after OER electrocatalysis was provided by Raman spectra showing a new peak at 550 cm<sup>-1</sup> (Figure S12), which were assigned as stretching vibrations corresponding to active NiOOH.

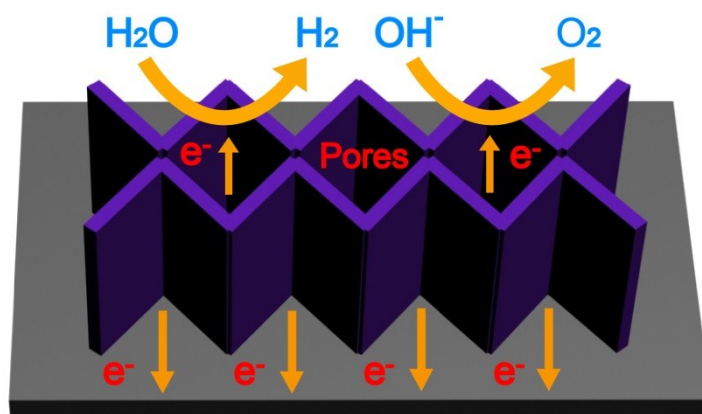


**Figure S13.** Schematic illustration of the operating principle of CF@NiP<sub>x</sub> bifunctional electrode.

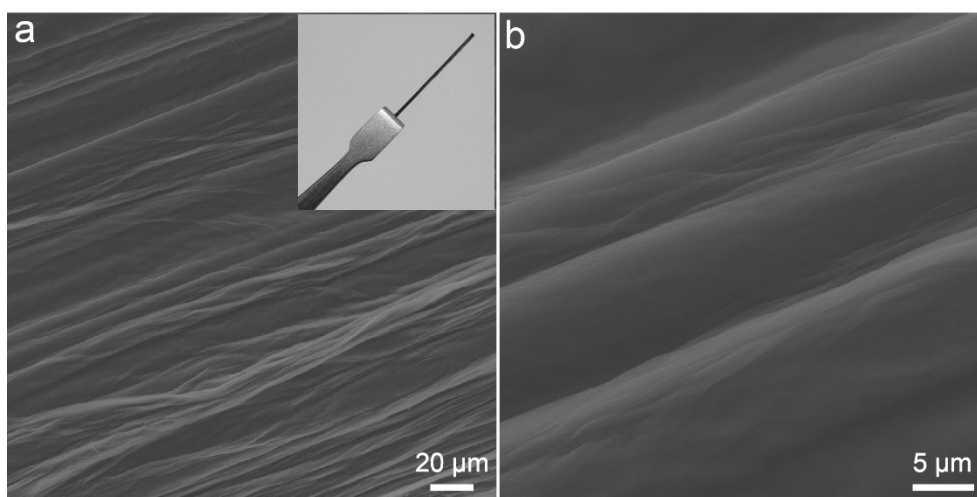


**Figure S14.** SEM images of our prepared CF@Ni@RGO (the inset shows a optical image of CF@Ni@RGO).

As shown in Figure S14a, a bundle of CFs were entirely wrapped with RGO film, and wrinkled features of the graphene nanosheets could be clearly observed from the high-magnification SEM image (Figure S14b), demonstrating the successful preparation of CF@Ni@RGO through our spontaneous redox reaction method.

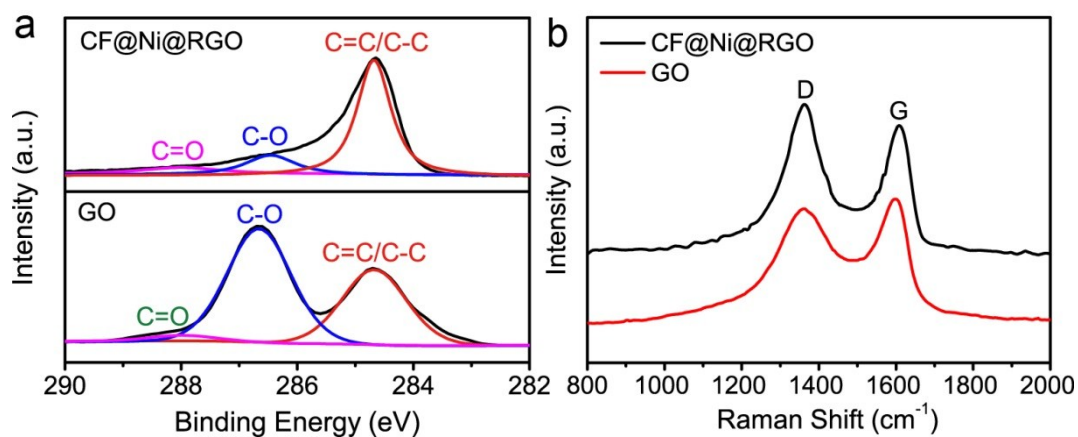


**Figure S15.** a) Deconvoluted C 1s XPS spectra and b) Raman spectra of GF@Ni@RGO and GO.

The deconvoluted C 1s XPS spectrum of CF@Ni@RGO (Figure S15a) shows three peaks for the graphitic structure (C=C/C-C at 284.6 eV), the hydroxyl/epoxy groups (C-O at 286.7 eV), and the carbonyl groups (C=O at 288.2 eV). Compared with the C 1s XPS spectrum of GO, the signals for the oxygen-containing groups in CF@Ni@RGO decrease significantly, demonstrating a high degree of deoxygenation and the successful reduction of GO during the immersion process. Similar results can also be found in the Raman spectrum (Figure S15b), the obvious increase in the intensity ratio of D to G peaks ( $I_D/I_G$ ) from 0.92 to 1.26 is observed due to the increase of  $sp^2$  domains in CF@Ni@RGO.

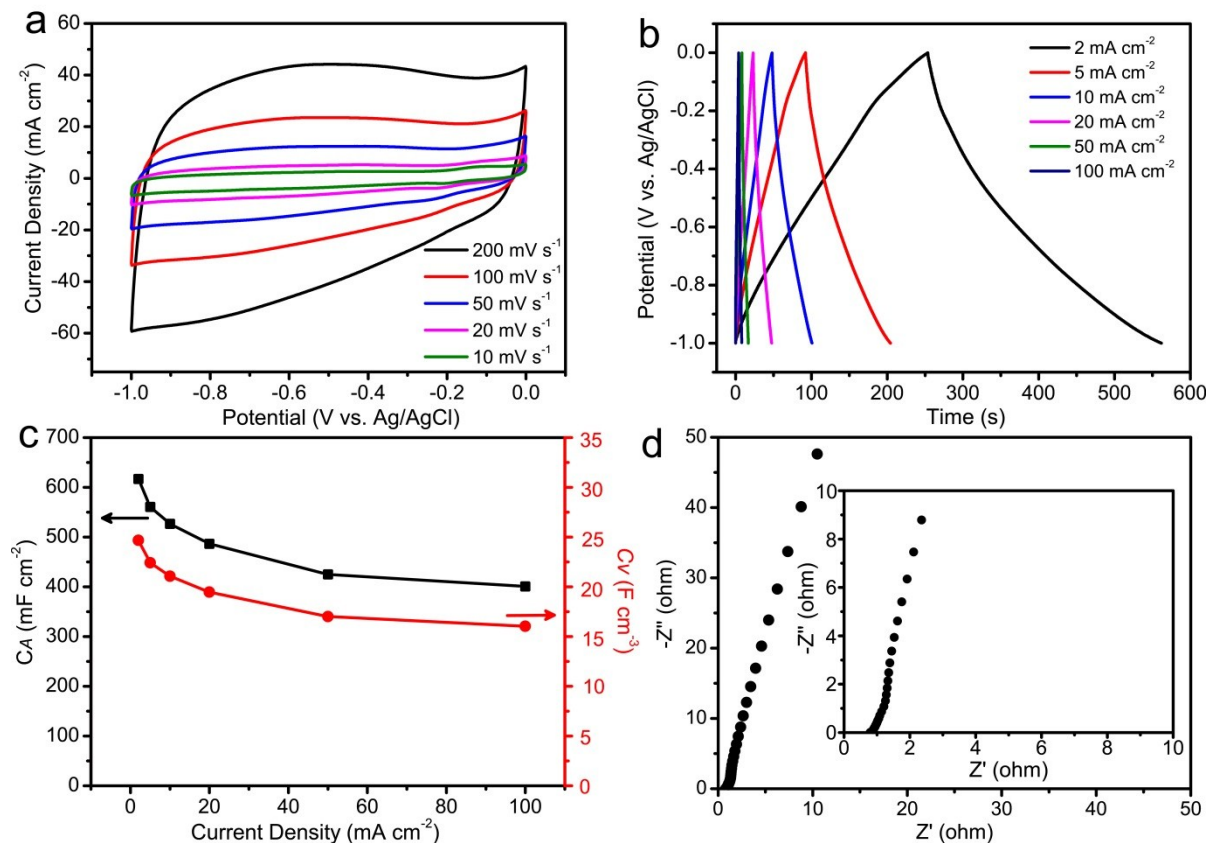


**Figure S16.** a) CV curves for the CF@Ni@RGO electrode at different scan rates in 6.0 M KOH. b) Galvanostatic charge/discharge curves for the CF@Ni@RGO electrode at different current density. c) Dependence of the areal and volumetric capacitances on the charge/discharge current density for the CF@Ni@RGO electrode. d) Nyquist plots of the CF@Ni@RGO electrode carried out in a frequency range from 10 mHz to 100 kHz (the inset shows the enlarged view of the high frequency region).

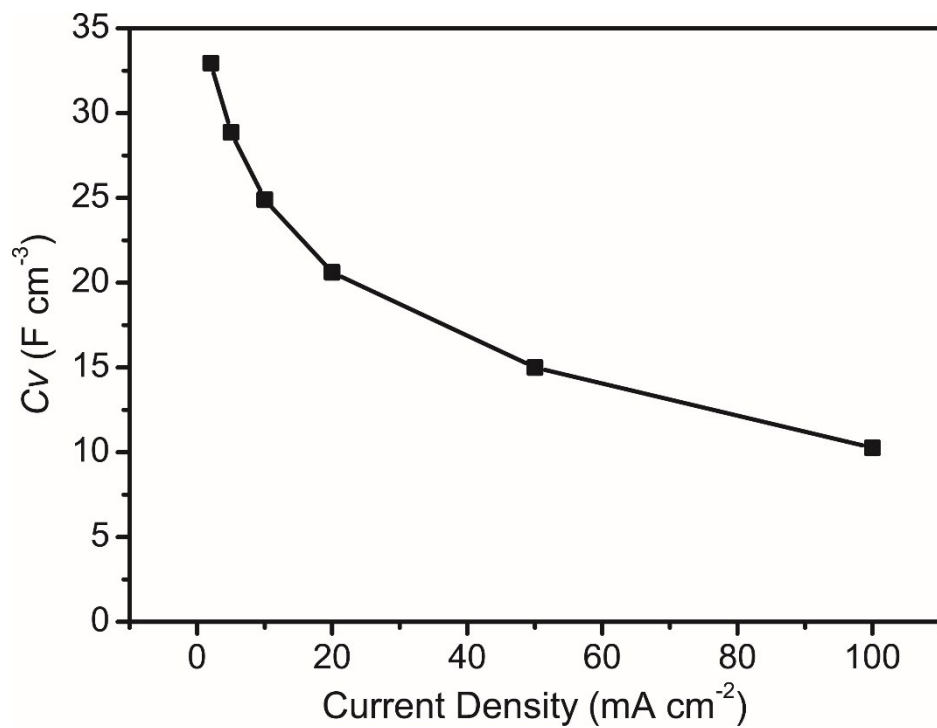


**Figure S17.** Specific volumetric capacitances of our prepared fiber-based solid-state asymmetric supercapacitor as a function of current density.

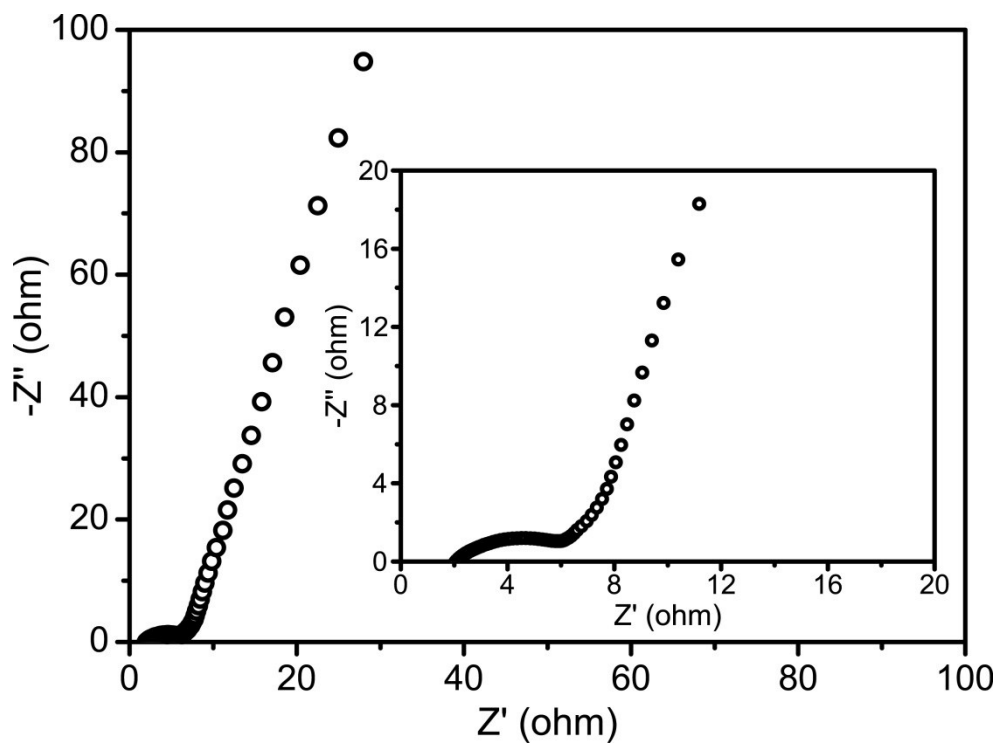


**Figure S18.** EIS spectrum of our prepared fiber-based solid-state asymmetric supercapacitor carried out in a frequency range from 10 mHz to 100 kHz (the inset shows the enlarged view of the high frequency region).

## 2. Supplementary Tables

**Table S1.** HER performance comparison of some non-precious metal-based catalysts.

Catalyst	Electrolyte	Tafel slope (mV dec <sup>-1</sup> )	$\eta_{10}$ (mV)	Reference
NiSe <sub>2</sub> nanoparticle/ carbon fiber paper	0.5 M H <sub>2</sub> SO <sub>4</sub>	50.1	139	J. Am. Chem. Soc. 2014, 136, 4897
THTNi <sub>2</sub> DSP sheet	0.5 M H <sub>2</sub> SO <sub>4</sub>	80.5	333	Angew. Chem. Int. Ed. 2015, 54, 12058
Ni <sub>5</sub> P <sub>4</sub> -Ni <sub>2</sub> P-NS	0.5 M H <sub>2</sub> SO <sub>4</sub>	79.1	120	Angew. Chem. Int. Ed. 2015, 54, 8188
Ni-Mo-S nanosheets	Neutral (PH~7)	85.3	200	Sci. Adv. 2015, 1, e1500259
Co/NG	1.0 M NaOH	—	~270	Nat. commun. 2015, 6,8668
MoB	1.0 M KOH	59	~219	Angew. Chem. Int. Ed. 2012, 51, 12703
Mo <sub>2</sub> C	1.0 M KOH	54	~190	Angew. Chem. Int. Ed. 2012, 51, 12703
Ni <sub>2</sub> P	1.0 M KOH	100	~228	Phys. Chem. Chem. Phys. 2014, 16, 5917
Ni-Mo/fluorine-doped tin oxide	1.0 M KOH	119	200	Angew. Chem. Int. Ed. 2015, 54, 664
<b>CF@NiP<sub>x</sub></b>	<b>1.0 M KOH</b>	<b>48.3</b>	<b>118</b>	<b>This work</b>

$\eta_{10}$ : current density @ 10 mA cm<sup>-2</sup>

**Table S2.** OER performance comparison of transition metal-based catalysts.

Catalyst	$\eta_{10}$ (mV)	Tafel slope (mV dec <sup>-1</sup> )	Electrolyte	Ref.
CoO/N-doped graphene	340	71	1.0 M KOH	Energy. Environ. Sci. 2014, 7, 609
Co <sub>3</sub> O <sub>4</sub> /N-doped-graphene	310	67	1.0 M KOH	Nat. Mater. 2011, 10, 780
Ni <sub>5</sub> P <sub>4</sub> /Ni foil	330	40	1.0 M KOH	Angew. Chem. Int. Ed. 2015, 54, 12361
Co-S/carbon tubes/carbon paper	306	72	1.0 M KOH	ACS Nano 2016, 10, 2342
Graphene-Co <sub>3</sub> O <sub>4</sub> nanocomposite	313	56	1.0 M KOH	Sci. Rep. 2015, 5, 7629
NiMo/Ti mesh	310	47	1.0 M KOH	J. Mater. Chem. A 2015, 3, 20056
Mn <sub>3</sub> O <sub>4</sub> /CoSe <sub>2</sub>	450	49	1.0 M KOH	J. Am. Chem. Soc. 2012, 134, 2930
NiFe ultrathin nanosheets	302	40	1.0 M KOH	Nat. commun. 2014, 5, 4477
NiCo ultrathin nanosheets	334	41	1.0 M KOH	Nat. commun. 2014, 5, 4477
<b>CF@NiP<sub>x</sub></b>	<b>200</b>	<b>54.7</b>	<b>1.0 M KOH</b>	<b>This work</b>

$\eta_{10}$ : current density @ 10 mA cm<sup>-2</sup>

**Table S3.** Volumetric capacitances comparison of various reported pseudocapacitor electrode materials.

Material	$C_v$ (F cm <sup>-3</sup> )	Electrolyte	Ref.
MoS <sub>2</sub> nanosheet	700	0.5 M H <sub>2</sub> SO <sub>4</sub>	Nature Nanotech. 2015, 10, 313
aMEGO/MnO <sub>2</sub>	640	1.0 M H <sub>2</sub> SO <sub>4</sub>	ACS Nano 2012, 6, 5404
GN/PANI/CNT	188	1.0 M HCl	Electrochim. Acta 2011, 56, 9224
Ti <sub>3</sub> C <sub>2</sub> T <sub>x</sub> paper	442	1.0 M KOH	Science 2013, 341, 1502
PANI/graphene composite	802	1.0 M H <sub>2</sub> SO <sub>4</sub>	Adv. Mater. 2015, 27, 8082
PPy-MnO <sub>2</sub> -CFs	70	0.5 M Na <sub>2</sub> SO <sub>4</sub>	Sci. Rep. 2013, 3, 2286
RGO-F/PANI	205	1.0 M H <sub>2</sub> SO <sub>4</sub>	J. Mater. Chem. A 2014, 2, 14413
<b>CF@NiP<sub>x</sub></b>	<b>817</b>	<b>6.0 M KOH</b>	<b>This work</b>